

Terahertz emission from vertically aligned InN nanorod arrays

H. Ahn, Y.-P. Ku, Y.-C. Wang, C.-H. Chuang, S. Gwo, and Ci-Ling Pan

Citation: [Applied Physics Letters](#) **91**, 132108 (2007); doi: 10.1063/1.2789183

View online: <http://dx.doi.org/10.1063/1.2789183>

View Table of Contents: <http://scitation.aip.org/content/aip/journal/apl/91/13?ver=pdfcov>

Published by the [AIP Publishing](#)

Articles you may be interested in

[Effect of Mg doping on enhancement of terahertz emission from InN with different lattice polarities](#)

Appl. Phys. Lett. **96**, 061907 (2010); 10.1063/1.3303983

[Electron accumulation at nonpolar and semipolar surfaces of wurtzite InN from generalized infrared ellipsometry](#)

Appl. Phys. Lett. **95**, 202103 (2009); 10.1063/1.3261731

[Intense terahertz emission from a -plane InN surface](#)

Appl. Phys. Lett. **92**, 102103 (2008); 10.1063/1.2892655

[Terahertz spectroscopic study of vertically aligned InN nanorods](#)

Appl. Phys. Lett. **91**, 163105 (2007); 10.1063/1.2800292

[Terahertz emission by InN](#)

Appl. Phys. Lett. **84**, 4810 (2004); 10.1063/1.1759385

The advertisement features a dark blue background with white and orange text. At the top left, it reads 'NEW! Asylum Research MFP-3D Infinity™ AFM' in large white letters, followed by 'Unmatched Performance, Versatility and Support' in orange. To the right is the Oxford Instruments logo, which includes the text 'OXFORD INSTRUMENTS' and 'The Business of Science®'. Below the main text are four images: a blue textured surface, a brown textured surface, a yellow and red patterned surface, and a photograph of the MFP-3D Infinity AFM instrument. Each image is accompanied by a short text description: 'Stunning high performance', 'Simpler than ever to GetStarted™', 'Comprehensive tools for nanomechanics', and 'Widest range of accessories for materials science and bioscience'.

Terahertz emission from vertically aligned InN nanorod arrays

H. Ahn,^{a)} Y.-P. Ku, Y.-C. Wang, and C.-H. Chuang

Department of Photonics, National Chiao Tung University, Hsinchu, Taiwan 30010, Republic of China and Institute of Electro-optical Engineering, National Chiao Tung University, Hsinchu, Taiwan 30010, Republic of China

S. Gwo

Department of Physics, National Tsing Hua University, Hsinchu, Taiwan 30013, Republic of China

Ci-Ling Pan

Department of Photonics, National Chiao Tung University, Hsinchu, Taiwan 30010, Republic of China and Institute of Electro-optical Engineering, National Chiao Tung University, Hsinchu, Taiwan 30010, Republic of China

(Received 30 May 2007; accepted 31 August 2007; published online 27 September 2007)

Terahertz emission from indium nitride (InN) nanorods and InN film grown by molecular-beam epitaxy on Si(111) substrates has been investigated. Terahertz emission from InN nanorods is at least three times more intense than that from InN film and depends strongly on the size distribution of the nanorods. Surface electron accumulation at the InN nanorods effectively screens out the photo-Dember field in the accumulation layer formed under the surface. The nanorods with considerably large diameter than the thickness of accumulation layer are found to be dominant in the emission of terahertz radiation from InN nanorod arrays. © 2007 American Institute of Physics.

[DOI: [10.1063/1.2789183](https://doi.org/10.1063/1.2789183)]

Indium nitride (InN) is an interesting and potentially important semiconductor material with superior electronic transport properties over other group-III nitrides.¹ Recently, low-dimensional InN nanomaterials in the forms of nanowires, nanorods, nanotubes, etc., have received great attention due to their potential in near-infrared (NIR) optoelectronics and as good candidates for photovoltaic materials. The discovery of the intrinsic narrow bandgap and remarkably large gap between the conduction band minimum and the next local minimum of InN also inspires potential applications in the terahertz range application, for example, as an efficient terahertz emitter/detector.

Recently, we have shown that vertically aligned InN nanorod arrays grown on silicon by plasma-assisted molecular-beam epitaxy (PAMBE) possess the crystal properties^{2,3} similar to wurtzite InN single crystal.⁴ The size distribution and the aerial (coverage) density of nanorods can be engineered by the growth conditions. It has been suggested that enhanced electron accumulation at the surface of the InN nanorods due to the high surface-to-volume ratio makes the InN nanorod array a promising material for NIR sensor applications.⁵

There have been several reports on terahertz emission from InN films.⁵⁻⁷ The terahertz radiation emitted from InN films is typically one order of magnitude weaker than that from InAs, although the main terahertz emission mechanism of both materials is the photo-Dember effect.⁸ In particular, Pradarutti *et al.*⁵ showed that terahertz emission from InN depends on the growth method and the surface morphology of samples. In their study, terahertz emission from an InN film with strong columnar morphology was found to be about one order of magnitude smaller than that from the InN film with smooth surface. Due to the increased effective

emitting surface area, however, nanostructured InN is expected to emit stronger terahertz signal than the epilayer. In this letter, we report the strong terahertz emission from vertically aligned InN nanorods grown along the wurtzite *c* axis by PAMBE on Si(111) substrates.² We found that terahertz radiation from InN nanorods strongly depends on the size and aerial density of the nanorods. Terahertz radiation due to the surface field in the very thin slab of the surface of InN film is typically much smaller than that due to the photo-Dember effect. However, for the nanorods with the diameter comparable to the thickness of the accumulation layer, terahertz radiation due to surface field cannot be neglected, significantly reducing the total terahertz amplitude.

For this work, three InN samples were grown on Si(111) substrates by PAMBE. The InN epilayer was grown on Si(111) using the epitaxial AlN/ β -Si₃N₄ double-buffer layer technique. Details of the growth procedure can be found elsewhere.⁹ The InN nanorods were grown at sample temperature of 330 °C [low-temperature grown nanorods (LT-NRs)] and 520 °C [high-temperature grown nanorods (HT-NRs)] on β -Si₃N₄/Si(111) (without the AlN buffer layer). The N/In flux ratios were ~ 2.6 and ~ 6.0 for LT-NR and HT-NR, respectively, and were adjusted at different growth temperatures to ensure that the growth proceeded in the columnar mode. The thicknesses of the InN epilayer, LT-NR, and HT-NR are ~ 2.5 μm , 750 nm, and 700 nm, respectively. The morphologies and size distribution of the InN nanorods were analyzed using field-emission scanning electron microscopy (FE-SEM). Terahertz emissions from photoexcited InN epilayer and nanorods were investigated using a Ti:sapphire regenerative amplifier laser system, which delivers ~ 50 fs optical pulses at a center wavelength of 800 nm with a repetition rate of 1 kHz. For this experiment, the photoexciting beam is collimated on the samples with a spot size of ~ 2 mm at the angle of incidence of 70°, which is near the Brewster angle. The emitted terahertz pulses were

^{a)} Author to whom correspondence should be addressed. Electronic mail: hyahn@mail.nctu.edu.tw

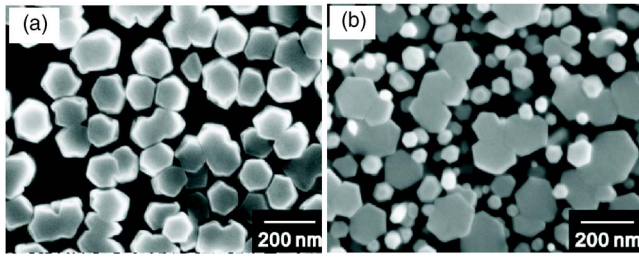


FIG. 1. (Color online) SEM images of vertically aligned (a) low-temperature-grown nanorods (LT-NRs) and (b) high-temperature-grown InN nanorods (HT-NRs), grown on Si(111) substrates by nitrogen-plasma-assisted molecule beam epitaxy. LT-NR has a uniform radius of 65 nm, while that of the HT-InN nanorods reveals a bimodal size distribution.

detected by free-space electro-optic sampling in a 2-mm-thick ZnTe crystal as a function of delay time with respect to the optical pump pulse.¹⁰ We have also investigated the azimuthal angle dependence of the terahertz emission, which reflects the contribution of the nonlinear effect.

The SEM image of the hexagonal-shaped LT-NR in Fig. 1(a) exhibits nanorods with a uniform diameter of ~ 130 nm, while that of the HT-NR in Fig. 1(b) reveals that besides the large-size nanorods, there are ultrasmall nanorods with an average diameter of ~ 60 nm filling up the spaces between larger-size (~ 130 nm) nanorods. The LT-NR exhibits an average aspect ratio (height/diameter) of ~ 6 and an aerial density of $\sim 5 \times 10^9 \text{ cm}^{-2}$. The average aspect ratios of the HT-NR are ~ 5.4 and ~ 12 for large and small nanorods, respectively, and the aerial density of HT-NR is $\sim 8 \times 10^9 \text{ cm}^{-2}$, including both modes.

Figure 2(a) shows the time-domain waveforms of terahertz emission for LT-NR (black line), HT-NR (red line), and the InN epilayer (blue line), respectively. Each sample is

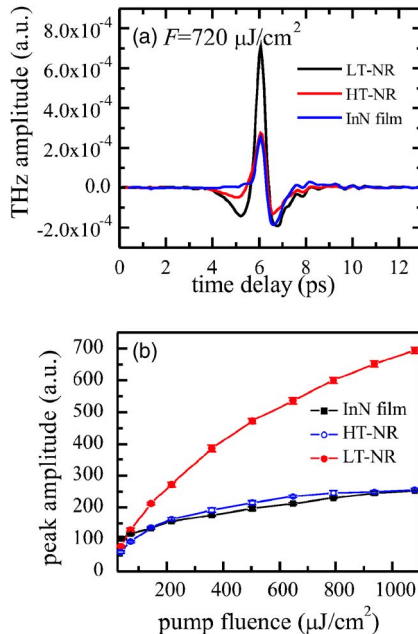


FIG. 2. (Color online) (a) Terahertz waveform generated from *n*-type InN film (blue), HT- (red), and LT-NRs (black), respectively. Each sample is excited at the fluence of $720 \mu\text{J}/\text{cm}^2$. (b) Peak amplitude of terahertz emission for InN film (solid squares), HT- (open circles), and LT-NRs (solid circles) as a function of laser pump power. Terahertz emissions from HT-NR and InN film begin to be nearly saturated from the low excitation level, while that from LT-NR keeps increasing with the excitation energy.

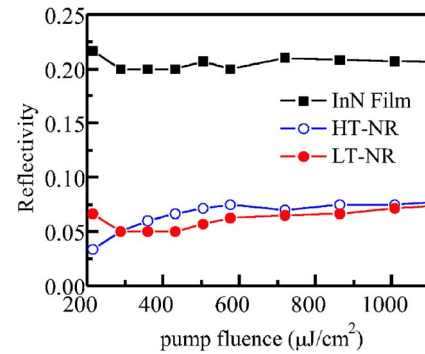


FIG. 3. (Color online) Optical reflectivities in HT-NR (open circles), LT-NR (solid circles), and InN film (solid squares) as a function of excitation energy. Optical absorption in InN film is about 80%, while that in nanorods is about 95%.

excited at the laser fluence of $720 \mu\text{J}/\text{cm}^2$. The dependence of the peak amplitude of terahertz emission on the pump power is plotted in Fig. 2(b). The peak terahertz amplitudes of the HT-NR and the InN film increase by about twice as the pump power increases by as much as ten times, while that of the LT-NR increases at least six times. Excited by laser pulses at $1 \text{ mJ}/\text{cm}^2$, the terahertz emission from LT-NR is about three times stronger than that from InN thin film and HT-NR.

Terahertz radiation from the narrow bandgap semiconductor is generated by the ultrafast-laser-driven accelerated carriers formed in a shallow surface area. Therefore, efficient terahertz emission from these materials is closely related to the near-surface characteristics of the materials, including their morphology, point defects, and the effective surface area. For InN film, since the surface accumulation layer is typically very thin (~ 10 nm) compared to the penetration depth of the laser pulse,¹¹ its contribution to the total terahertz radiation is negligible compared to the photo-Dember effect.^{5,6} Moreover, for *n*-type InN with a high carrier concentration, the direction of surface field is opposite to the photo-Dember field and consequently reduces the total magnitude of the terahertz radiation. Room-temperature polarized Raman spectroscopic studies³ showed that the concentrations of free carriers in nanorods are one order of magnitude higher than that in the InN film, suggesting that there are considerable amounts of structural defects in the LT-NR. Further, room-temperature photoluminescence signals of HT-NR and LT-NR are about one to two orders of magnitude lower than that of the InN film.² This phenomenon has been attributed to strong surface electron accumulation effect, which screens photocarriers and in turn reduces the radiative recombination in InN nanorods.

Nanorods have drastically increased effective surface area compared to the film and every surface exposed to the photoexcitation pulses may participate in the absorption. In order to investigate the relation between the surface area and optical absorption, we studied the reflectance of each sample. Measured nearly-normal-incident reflectance in Fig. 3 demonstrates that over the whole range of excitation level, absorption in nanorods ($\sim 95\%$) is much larger than that in the film ($\sim 80\%$). And it may correspond to the enhanced optical absorption in nanorods by increased effective surface area. Here, one must notice that HT-NR absorbs as much of excitation energy as LT-NR does, while terahertz radiation from HT-NR in Fig. 2 is much lower than that from LT-NR. This

inefficient conversion of optical absorption to terahertz emission in HT-NR may be understood by the nanorod-size dependence of terahertz emission. Since the penetration depth of the laser pulse in the nanorod is limited by its geometrical shape, the surface-to-volume ratio becomes the crucial factor for the optical absorption and terahertz emission.

The radius of large-size nanorods formed in both LT- and HT-NR is about 65 nm. This is smaller than the penetration depth of the laser pulse but still larger than the surface accumulation layer. Since the surface field is opposite in direction to the photo-Dember field, if we exclude the accumulation layer (~ 10 nm) from the total volume of nanorods, terahertz radiation by the photo-Dember field is mainly generated in the inner volume with the radius of ~ 55 nm. Meanwhile, the ultrasmall nanorods in HT-NR have much smaller radius (~ 30 nm) and their effective volume of terahertz radiation is as small as the inner volume with the radius of 20 nm. Under the assumption that terahertz emission from surface accumulation layer is negligible because of screening, we can roughly calculate the effective volume of terahertz emission by the nanorods solely due to the photo-Dember effect. Compared with LT-NR, the number of large-size nanorods of HT-NR reduces by $\sim 40\%$ [see FE-SEM images in Fig. 1(b)]. On the other hand, there is about three times more number of ultrasmall nanorods with small effective volume closely packing the space between large-size nanorods. Although there are much more nanorods including both large-size and ultrasmall rods, the total effective volume of terahertz emission for HT-NR is about twice smaller than that for LT-NR. As the excitation power increases, the absorption and terahertz emission in LT-NR increase accordingly due to its large effective volume. In contrast, the increased absorption in the ultrasmall nanorods of HT-NR may not be effectively converted into terahertz emission due to the decreased effective volume.

Although the azimuthal angle dependence of terahertz emission from both LT- and HT-NRs shows only small modulation amplitude (few percents of total amplitude), non-linear dependence of terahertz emission on pump fluence for

LT- and HT-NRs [see Fig. 2(b)] implies that additional non-linear effects might still play a role in both materials, especially for the LT-NR. Further study is under investigation.

In summary, we demonstrated that the InN nanorods emit terahertz wave more than three times stronger than that of the InN film. The “screened” photo-Dember effect is found to be the main terahertz emission mechanism of InN nanorods. The enhancement of terahertz emission is closely related to the surface-to-volume ratio of the nanorods. Nanorods with the radii smaller or comparable to the thickness of the accumulation layer do not contribute significantly to terahertz emission.

This work was supported in part by the National Science Council (NSC) through various grants including NSC 96-2112-M-009-016-MY3, PPAEU-II, and the ATU program of the Ministry of Education, Taiwan, R. O. C.

- ¹A. G. Bhuiyan, A. Hashimoto, and A. Yamamoto, *J. Appl. Phys.* **94**, 2779 (2003), and references therein.
- ²C.-H. Shen, H.-Y. Chen, H.-W. Lin, S. Gwo, A. A. Klochikhin, and V. Yu. Davydov, *Appl. Phys. Lett.* **88**, 253104 (2006).
- ³H.-Y. Chen, C.-H. Shen, H.-W. Lin, C.-H. Chen, C.-Y. Wu, S. Gwo, A. A. Klochikhin, and V. Yu. Davydov, *Thin Solid Films* **515**, 961 (2006).
- ⁴H. Ahn, C.-H. Shen, C.-L. Wu, and S. Gwo, *Appl. Phys. Lett.* **86**, 201905 (2005).
- ⁵B. Pradarutti, G. Matthaus, C. Bruckner, S. Riehemann, G. Notni, S. Nolti, V. Cimalla, V. Lebedev, O. Ambacher, and A. Tunnermann, *Proc. SPIE* **6194**, 619401 (2006).
- ⁶R. Ascazubi, I. Wilke, K. Denniston, H. L. Lu, and W. J. Schaff, *Appl. Phys. Lett.* **84**, 4810 (2004).
- ⁷G. D. Chern, E. D. Readinger, H. Shen, M. Wraback, C. S. Gallinat, G. Koblmüller, and J. S. Speck, *Appl. Phys. Lett.* **89**, 141115 (2006).
- ⁸M. C. Nuss and J. Orenstein, in *Millimeter and Submillimeter Wave Spectroscopy of Solids*, edited by G. Gruner (Springer, Berlin, 1998), p. 7.
- ⁹S. Gwo, C.-L. Wu, C.-H. Shen, W.-H. Chang, T. M. Hsu, J.-S. Wang, and J.-T. Hsu, *Appl. Phys. Lett.* **84**, 3765 (2004).
- ¹⁰T.-R. Tsai, C.-Y. Chen, C.-L. Pan, R.-P. Pan, and X.-C. Zhang, *Appl. Opt.* **42**, 2372 (2003).
- ¹¹I. Mahboob, T. D. Veal, L. F. J. Piper, C. F. McConville, Hai. Lu, W. J. Schaff, J. Furthmüller, and F. Bechstedt, *Phys. Rev. Lett.* **92**, 036804 (2004).